

Heterogeneity-Aware Client Selection Methodology For Efficient Federated Learning

Nihal Balivada¹, Shrey Gupta², Shashank Shreedhar Bhatt³, Suyash Gupta¹

¹ University of Oregon, US, ² Boston College, US, ³ Microsoft Research, India

Abstract

Federated Learning (FL) enables a distributed client-server architecture where multiple clients collaboratively train a global Machine Learning (ML) model without sharing sensitive local data. However, FL often results in lower accuracy than traditional ML algorithms due to statistical heterogeneity across clients. Prior works attempt to address this by using model updates, such as loss and bias, from client models to select participants that can improve the global model’s accuracy. However, these updates neither accurately represent a client’s heterogeneity nor are their selection methods deterministic. We mitigate these limitations by introducing Terraform, a novel client selection methodology that uses gradient updates and a deterministic selection algorithm to select heterogeneous clients for retraining. This bi-pronged approach allows Terraform to achieve up to 47% higher accuracy over prior works. We further demonstrate its efficiency through comprehensive ablation studies and training time analyses, providing strong justification for the robustness of Terraform.

1 Introduction

In this paper, we present **Terraform**, a novel client selection methodology for Federated Learning (FL) McMahan *et al.* [2017] that addresses heterogeneity in client data distribution by iteratively partitioning clients into two clusters, easy and hard, based on a split index. An FL framework enables a distributed client-server architecture Tanenbaum and van Steen [2007] where multiple clients collaboratively train a *global* Machine Learning (ML) model without sharing sensitive (local) data. Each client receives the global model’s parameters from the server, uses them to train the model on its data, and shares the updated model parameters with the server. Consequently, the server aggregates the parameters from various clients. This process continues until the global model reaches convergence (highest accuracy).

Despite significant seminal research in FL Yang *et al.* [2019], its practical adoption remains limited due to its lower accuracy yields compared to traditional ML algorithms. This

is because the local data of clients is often drawn from different distributions, causing *statistical heterogeneity* Chen and Vikalo [2024]. In an FL environment, statistical heterogeneity represents the variation in data distributions across clients, caused by the variations in feature or label distributions of clients’ local data. It contributes to the non-iid (non-independent & identically distributed) nature of the data.

Statistical heterogeneity is a double-edged sword; while it improves model generalization due to data diversity, it increases training complexity and reduces model accuracy. For example, modeling air quality requires training an ML model on environmental features, such as weather conditions and the topography of the location of interest Cheng *et al.* [2018]. Coincidentally, several organizations perform such an air quality modeling on a global scale that spans multiple countries Galmarini and Trivikrama Rao [2011]; Pan *et al.* [2017]. However, globally scaling these models requires data sharing, which is challenging due to proprietary concerns or national security. FL is an ideal candidate for training such a model, as it enables localized data collection and training. Unfortunately, FL inadvertently induces statistical heterogeneity, as in this example – one training location may be an urban area with high pollutant emissions, while another is in a rural setting. Although this heterogeneity generalizes the global model, it increases the probability of capturing unwanted patterns, reducing model performance.

Prior works attempt to mitigate the negative impact of statistical heterogeneity by designing client selection methodologies that decide which clients should participate in FL training. Lai *et al.* [2021] estimate the statistical utility of each client based on multiple factors like model loss, device speed, and bandwidth, and then randomly select a subset of high utility clients for retraining. Jee Cho *et al.* [2022] select “ m ” clients with highest local training loss for retraining, where the value of m is determined by the system. In contrast, Chen and Vikalo [2024] cluster clients into groups using their final layer’s biases and retrain clients in those clusters that have more uniform data distributions.

Although these prior works present valuable designs, they are unable to attain higher accuracy for the following two reasons: (i) they assume client updates are either losses or final-layer biases, which do not reveal all details about a client’s data distribution; and (ii) their algorithms for selecting clients to be retrained are not deterministic. In contrast, our method-

ology, **Terraform**, aims to **eliminate randomness** by deterministically selecting which clients need retraining and utilizing **updates that precisely account for statistical heterogeneity**. Additionally, Terraform ensures that it does **not introduce any new computational or communication costs**.

So how does Terraform meet these goals? Terraform’s novel client selection methodology expects each client to send the **final-layer gradient updates** returned by its model after training and the **dataset size**, which capture statistical utility of a client’s data. Terraform uses gradient updates to **sort the clients** and the dataset size to determine the **Inter-Quartile Range**, which enables us to find an optimal **split index** to partition clients into two clusters: **easy** and **hard**. Terraform **selects and retrains** clients in the hard cluster (iterates over the above steps in the process) till only a *threshold* number of clients remain.

To ensure that Terraform does perform in practice, we follow prior works and implement it in two popular FL algorithms, FedAvg and FedProx, and extensively compare Terraform against five state-of-the-art client selection methodologies. Our results illustrate that Terraform outperforms all the client sampling techniques on the five popular FL datasets (FEMNIST, CIFAR10, CIFAR100, FMNIST, and Tiny ImageNet) and increases accuracy of FedAvg and FedProx by up to 47% and 41%, respectively. Additionally, we validate robustness of Terraform’s design through rigorous ablations and training time experiments.

2 The Case for Data Heterogeneity

We motivate the need to tackle client data heterogeneity through the following example. US communities regularly face disproportionate threats of disasters like wildfires and fire incidents Federal Emergency Management Agency [1997]; Rivers and University [2022]; National Interagency Coordination Center (NICC) [2024]. In response, US government has accelerated installation of IoT wildfire sensors like PTZ Camera University of Nevada *et al.* [2025], promoted use of smart home sensors like Google Nest LLC [2025], and funded setup of Hazard workflows like AlertWildfire Smith *et al.* [2016]. These hazard workflows collect observations with sensors, disseminate those observations to remote cloud for processing, infer the impacts of those hazards at cloud, and notify various stakeholders. However, these hazard workflows face two major challenges: (i) they collect user data through sensors and upload them to the cloud, which violates user privacy of Homeland Security [2013]; Raffeg and others [2025]; Wall and Space.com [2025]; U.S. Department of Homeland Security [2019], and (ii) they consume massive network bandwidth due to sensor-cloud communication. This presents an elegant opportunity to leverage FL for disaster response Jin and Du [2024]; the sensors can play the role of clients and participate in FL training.

Notice that the two type of sensors we consider here, PTZ camera and Google Nest, have distinct deployment range and alert frequency. PTZ cameras are sparse, remote (often in forests), and generate few but highly reliable wildfire alerts. Nest sensors, on the other hand, are abundant in homes and produce frequent non-wildfire alerts with rare true positives

due to smoke from wood stoves, prescribed burns, vehicles, etc. Since most training data comes from home sensors, any FL system that does not account for data heterogeneity will overlook the true positive alerts from the cameras, causing the global model to have low accuracy and missing early wildfire signals.

Terraform aims to train on these heterogeneous data and ensure that it yields high accuracy for all the events.

3 Background

The seminal FedAvg algorithm McMahan *et al.* [2017] coined the term Federated Learning (FL), where in a distributed client-server architecture, multiple clients collaboratively train a global ML model without sharing local data with the server. We formalize its design as follows:

Consider a standard FL system where a server coordinates K participating clients, indexed by $k = \{1, 2, \dots, K\}$. Each k -th client has a local classification dataset (used for training), $D_{\text{train}}^k = \{(x_j^{(k)}, y_j^{(k)})\}$, where $x_j^{(k)} \in \mathbb{R}^m$ is the feature vector, and $y_j^{(k)} \in \{1, \dots, C\}$ are the labels with C classes. Each client computes a model update by minimizing loss function $L(\theta; x_j^{(k)}, y_j^{(k)})$ where θ denotes the model parameters. These updates are sent to the server, which performs weighted averaging over the received updates, where weights are proportional to each client’s dataset size, $|D_{\text{train}}^k|$; this leads to updated global model parameters. The server then shares the updated model parameters with the clients, and this process continues for either a pre-defined number of rounds or until the model reaches an accuracy saturation. The accuracy of the global model is evaluated on each client’s test data, D_{test}^k .

Techniques addressing statistical heterogeneity Prior works have explored a variety of approaches to handle statistical heterogeneity in federated learning (FL). **Regularization-based** techniques discourage client model drift from the global solution by modifying the local objective. For example, FedProx Li *et al.* [2020] adds a proximal term for more stable convergence, while FedDyn Acar *et al.* [2021] aligns the global and client optima via a dynamic regularizer, and FedDC Gao *et al.* [2022] uses an auxiliary variable to decouple and correct gradient and parameter drift by tracking local drift. **Variance reduction and drift correction** algorithms like SCAFFOLD Karimireddy *et al.* [2020] remove client drift and achieve comparable convergence rates to centralized SGD using control variates, while FedNova Wang *et al.* [2020b] eliminates objective inconsistency due to heterogeneity in the number of local updates by normalizing the client updates. Other algorithms like VRL-SGD Liang *et al.* [2020], FedVRA Wang *et al.* [2023] and FedRed Jiang *et al.* [2024] reduce variance via gradient tracking or dual variables. **Adaptive optimization and dynamic aggregation** methods improve performance under statistical heterogeneity by extending techniques from adaptive optimizers like Adagrad, Adam and Yogi to the federated setting Reddi *et al.* [2021]. For example, FedAW Tang [2024], FedAWA Shi *et al.* [2025] and FedADp Wu and Wang [2021] make use of client contributions to adaptively adjust aggrega-

tion weights. **Layer-wise and architecture-aware aggregation** methods such as FedMA Wang *et al.* [2020a] use neuron-matching and averaging to improve performance on deep CNN and LSTM architectures. **Contrastive approaches** like MOON Li *et al.* [2021a] align global and local representations using contrastive losses.

Personalization / multi-mode techniques tackle statistical heterogeneity via knowledge preserving cross-client transfer and create models tailored for each client. These techniques include using locally regularized models personalization (Ditto Li *et al.* [2021b] with local copies and pFedMe T Dinh *et al.* [2020] with Moreau envelopes), meta learning for fast adaptation (PeFLL Scott *et al.* [2024], Per-FedAvg / MOCHA Fallah *et al.* [2020] and federated MAML Jiang *et al.* [2019]), representation decoupling (LG-FedAvg Liang *et al.* [2019], FedPer Arivazhagan *et al.* [2019], FedRoD Chen and Chao [2022] and FedRep Collins *et al.* [2021]), parameter/feature alignment (FedAS Yang *et al.* [2024] and FedPAC Xu *et al.* [2023]), bilevel optimization methods (pFedHN Shamsian *et al.* [2021] and FedBabu Oh *et al.* [2022]), and partitioning the hypothesis space into compatible submodels (FLOCO Grinwald *et al.* [2024] with solution-simplex methods). **Clustered and model-mixture** methods cluster clients based on similarity (e.g., FedClust Islam *et al.* [2024], CFL Sattler *et al.* [2020], and IFCA Ghosh *et al.* [2020]) and train a model for each cluster. **Data augmentation and distillation** techniques like FedDF Lin *et al.* [2020], FedMD Li and Wang [2019], FedMix Yoon *et al.* [2021], FedFed Yang *et al.* [2023], FedProto Tan *et al.* [2021] and FADA Peng *et al.* [2020] reduce data statistical heterogeneity by using proxy data or shared statistics.

Finally, **client selection and sampling** techniques balance efficiency and representativeness by systematically picking the clients participating in each round of federated training. These techniques prioritize clients based on a quantification of their utility — statistical PoW-D Jee Cho *et al.* [2022], system-based (FedCS Nishio and Yonetani [2019]), or both (Oort Lai *et al.* [2021]) — towards the expected progress per round. They also consider the diversity or correlation between client updates (DivFL Balakrishnan *et al.* [2022] and FedCor Tang *et al.* [2022]) and population structure captured by clustered sampling Fraboni *et al.* [2021], including advanced hierarchical variants like HiCS-FL Chen and Vikalo [2024], which additionally uses output-layer bias update information for heterogeneity-aware client selection.

4 Related Work

Client Selection Methodologies. The FedAvg algorithm selects participating clients randomly in each training round. However, this random selection can lead to client drift—a phenomenon in which the global model either converges slowly or becomes trapped in local optima, often due to the repeated selection of highly heterogeneous clients in each round Karimireddy *et al.* [2020]. FedProx Li *et al.* [2020] extends FedAvg and addresses client drift by adding a regularization term that penalizes large deviations from the global model. This keeps the local updates more aligned with the global optima as well as improves the stability in model train-

ing. As a result, a broad body of federated learning research focuses on designing principled client selection methodologies that can recognize client heterogeneity and concentrate retraining efforts on the most impactful clients.

Lai *et al.* [2021] introduce *Oort*, which estimates the statistical utility of each client in FL training based on how effectively its updates improve the global model. This utility is measured as a combination of model loss, device speed, and bandwidth, and helps to assign each client a selection probability. *Oort* sorts the clients based on these probabilities and randomly selects a subset of high-probability clients. Additionally, it randomly selects a few low-probability clients to reduce training bias. Jee Cho *et al.* [2022] introduce *power of choice (PoC)*, which selects clients with high local training loss. The server first randomly samples a pool of candidate clients and queries their local training loss. Next, it selects m clients with the highest losses, where the value of m is determined by the system. *HiCS-FL* Chen and Vikalo [2024] uses bias values from the final layer of client models to determine the complexity of its dataset. It uses these biases to cluster clients into groups, assigns them a sampling probability, and trains clients in clusters with high sampling probability. Specifically, *HiCS-FL* targets clients with less complexity, which is opposite to our goal. Note: while *PoC* and *Oort* use loss as client updates, *HiCS-FL* uses biases. Further, these protocols do not collect updates in each round, which makes them outdated and prevents them from giving a holistic representation of the client’s local model.

In contrast, Terraform requires clients to send final-layer *gradient updates*, which is the sum of both weights and biases, to compute a client’s statistical heterogeneity. These gradient updates are a better indicator of the client’s distribution due to their proximity to the output layer, and they capture a more direct signal than loss of how well a client’s model has learned Zeiler and Fergus [2014].

Hierarchical Splitting. The hierarchical selection approach in Terraform is inspired by the CART (Classification and Regression Trees) model Breiman *et al.* [1984], which recursively partitions data at decision nodes into *left* and *right* child nodes using a partitioning criterion. Hierarchical sampling has also been applied in the meta-learning setting for spatio-temporal domains Xie *et al.* [2021]; Liu *et al.* [2023], where prior works focus on applying hierarchical splitting in a centralized setup. In contrast, Terraform introduces hierarchical splitting in a federated (i.e., distributed) learning setting, where only gradients are exchanged between clients and the server—minimizing communication overhead and preserving privacy. Furthermore, Terraform explicitly accounts for local dataset heterogeneity during client-side training, improving model performance in non-iid scenarios.

5 Terraform Overview

Terraform is a novel client selection methodology, which when employed by an existing federated learning (FL) algorithm helps it to select statistically heterogeneous clients that negatively impact the accuracy of the FL algorithm. We use Figure 1 to illustrate the design of Terraform.

Like any other methodology, Terraform requires rounds to

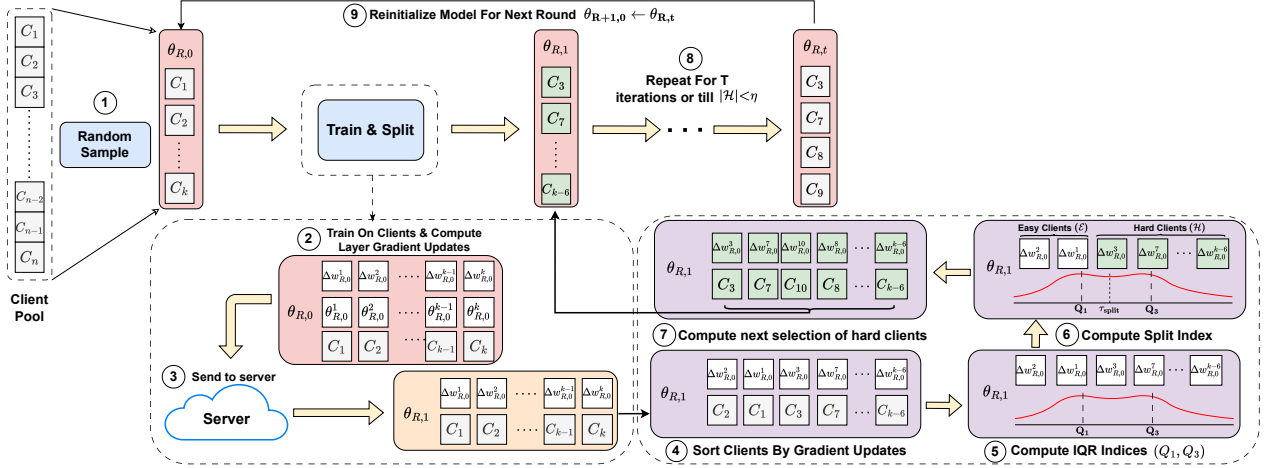


Figure 1: Terraform Framework.

train the clients. However, each round of Terraform performs hierarchical client selection through a series of iterations. A single iteration of Terraform includes the following steps. The server starts with the global model¹ and sends its parameters to a subset of clients, selected uniformly at random (Step 1 in Figure 1 \rightarrow ①). Next, each client locally trains this model on its dataset ②, after which it sends the final-layer gradients of the model to the server ③. Upon receiving these gradients from all selected clients, the server aggregates them and begins the process of identifying statistically heterogeneous clients. To do so, the server first sorts the clients based on the values of their gradients ④. Next, it uses the dataset size of each client to determine the inter-quartile range (IQR), which is the difference between the third and first quartile, representing 50% of the gradient magnitudes ⑤. Within this IQR, the server determines the split index that partitions the clients into easy and hard clusters ⑥. The server initiates retraining of the clients in the hard cluster (initiating the next iteration) by forwarding them aggregated gradients, and these clients again undergo the above steps ⑦. In essence, this process continues until the number of clients in the hard cluster falls below a predefined threshold ⑧.

6 Methodology

We denote the FL algorithm employing Terraform as \mathcal{A} , the initial global model at the server \mathcal{S} as $\theta_{0,0}$, and the number of training rounds as R . In each round, $r \in \{0, \dots, R-1\}$, \mathcal{S} randomly samples K clients, forming the client pool \mathcal{C}_r^K .

Within each round, Terraform performs at most T iterations, $T \geq 1$. The updated global model parameters at the end of the t -th iteration are $\theta_{r,t}$. Within each iteration, the clients are split into an easy cluster \mathcal{E} and a hard cluster \mathcal{H} based on a split index, τ_{split} , which is determined using the client’s gradient update, $\Delta w_{r,t}^k$, and its dataset size, $|D_{train}^k|$; where k represents a client.

The split index, τ_{split} , is selected from the client indices falling between the first (Q_1) and third (Q_3) quartiles of

the distribution of dataset sizes, $|D_{train}^k|$. Hence, Terraform searches for an optimal split index to generate two groups – one on which the global model approximates easily (low $|\Delta w_{r,t}^k|$, i.e., easy cluster, \mathcal{E}) and the other on which the global model struggles to approximate (high $\Delta w_{r,t}^k$, i.e., hard cluster, \mathcal{H}). Terraform continues this round until the number of clients in the hard cluster falls below the predefined threshold, η .

Next, we explain in detail Terraform’s client selection methodology and use Algorithm 1 to illustrate its algorithm.

6.1 Client Model Updates

In contrast to prior work that relies on losses or final-layer biases for client selection, Terraform leverages final-layer gradients, as these provide deeper insights into the underlying data distribution of each client (refer to Figure 2). As illustrated in Figure 1, in an iteration t of a round r , the client k performs training on its local data D_{train}^k using the global model parameters $\theta_{r,t}$, which generates the local model parameters, $\theta_{r,t}^k$ such that:

$$\theta_{r,t}^k \leftarrow \theta_{r,t} - \Delta w_{r,t}^k \quad (1)$$

where $\Delta w_{r,t}^k$ is the gradient update between $\theta_{r,t}$ and $\theta_{r,t}^k$ due to local training and includes both the weight and bias matrices obtained from the model’s final layer (also called the classification layer) Zeiler and Fergus [2014]. The magnitude of the gradient updates $|\Delta w_{r,t}^k|$ and the dataset size, $|D_{train}^k|$, are returned to the server. The magnitude of a client’s total gradient update, $|\Delta w_{r,t}^k|$, is obtained by taking the square root of the sum of the squared Frobenius norms Golub and Van Loan [1996] of its final layer’s individual parameters’ gradient update, Δp_i^k :

$$|\Delta w_k| = \sqrt{\sum_{i=1}^L \|\Delta p_i^k\|_F^2} \quad (2)$$

where L is the number of trainable parameters in the final layer. The Frobenius norm of a matrix $\mathbf{A} \in \mathbb{R}^{m \times n}$ tells us

¹Like prior works, we generate the initial global model through random initialization Li *et al.* [2020].

the size of \mathbf{A} , and is given by the square root of the summed absolute squares of its elements:

$$\|\mathbf{A}\|_F = \sqrt{\sum_{i=1}^m \sum_{j=1}^n |a_{ij}|^2} \quad (3)$$

Intuitively, the gradient updates indicate how much new information the client’s data is adding to the global model. A small gradient update suggests that the global model requires less fine-tuning on the client’s data, that is, the client’s data distribution aligns with the data distribution learned by the global model.

6.2 Hierarchical Selection

Terraform’s hierarchical selection takes inspiration from the Classification and Regression Trees (CART) algorithm, which constructs a binary decision tree by recursively partitioning data at each node into *left* and *right* child nodes based on a partitioning criterion. For classification tasks, well-known partitioning criteria like Gini index and Entropy Hastie *et al.* [2001] are employed, whereas for regression tasks, the Sum of Squared Errors (SSE) method is used. For example, assume a regression problem that needs to generate a CART decision tree. The partition at each node n_i of the tree, where $n_i \in \{1, \dots, N\}$ is determined using the total SSE of the resulting child nodes defined as $\text{SSE}(N_L)$ and $\text{SSE}(N_R)$. It equates to, $\text{SSE}(N_L) = \sum_{n_i \in N_L} (n_i - \bar{n}_L)^2$, where \bar{n}_L represents the mean of the left partition; and similarly for the right partition. CART selects the partition that minimizes the total SSE for each node, $\text{SSE}_{\text{total}} = \text{SSE}(N_L) + \text{SSE}(N_R)$.

Terraform’s hierarchical selection extends these rules to the FL environment such that a client’s gradient update magnitude $|\Delta w_{r,t}^k|$ represents a node. These gradients are used to calculate the split index that partitions them into two clusters: easy \mathcal{E} and hard \mathcal{H} . However, finding the optimal split index from this large set of gradient magnitudes is hard. Thus, Terraform introduces the notion of Inter-Quartile Range (IQR), explained next.

Inter-Quartile Range (IQR).

Prior to calculating the split index, Terraform sorts the clients based on the magnitude of their gradient updates $|\Delta w_{r,t}^k|$. Once the clients are sorted, their dataset sizes, $|D_{\text{train}}^k|$, are used to calculate the running sum, $S_k = \sum_{j=1}^k |D_{\text{train}}^j|$, where S_k denotes the cumulative dataset size up to the k -th client in the list. This running sum is used to identify a subset of clients that can optimize the calculation of the split index, which we denote as the *Inter-Quartile Range* (IQR).

The IQR is the difference between the third quartile (Q3) and the first quartile (Q1), representing the middle 50% of the data. It captures the central distribution of the gradient magnitudes, thereby excluding outliers. To locate the first quartile index k_{Q1} , we find the smallest k such that $S_k \geq 0.25 \cdot S_K$, where S_K is the total running sum. Similarly, the third quartile index k_{Q3} is the smallest k such that $S_k \geq 0.75 \cdot S_K$. In Figure 3, we empirically validate the calculation of the split index with and without IQR.

Split Index.

To calculate the optimal split index, we consider it as a problem of splitting a list of scalar values $U = \{u_1, \dots, u_i, \dots, u_N\}$, where u_i corresponds to gradient magnitude, $|\Delta w_{r,t}^i|$; these are sorted in ascending order, into two distinct subsets. Xie *et al.* [2021] shows that the optimal split index τ_{split} can be obtained by minimizing the variance within the two resulting clusters, which we define as *intra-split variance*, $\text{Var}_{\text{intra}}$. Based on this, the optimal splitting index, τ_{split} can be defined as,

$$\tau_{\text{split}} = \underset{1 \leq \tau < N}{\text{argmin}} (\text{Var}_{\text{intra}}(U_1, U_2)) \quad (4)$$

where $U_1 = \{u_1, \dots, u_\tau\}$, $U_2 = \{u_{\tau+1}, \dots, u_N\}$ are the clusters of U after splitting at a given split index τ . Furthermore, we can define $\text{Var}_{\text{intra}}$ as,

$$\text{Var}_{\text{intra}}(U_1, U_2) = \frac{|U_1|}{N} \cdot \text{Var}(U_1) + \frac{|U_2|}{N} \cdot \text{Var}(U_2) \quad (5)$$

where $\text{Var}(U) = \frac{1}{S_N} \sum_{i=1}^N (|D_{\text{train}}^i| \cdot (u_i - \bar{u})^2)$ is the variance of the cluster, $\bar{u} = \frac{1}{S_N} \sum_{i=1}^N |D_{\text{train}}^i| \cdot u_i$ is the mean of the cluster, S_N is the total running sum and N is the total number of cluster elements. Hence, the problem is reduced to an iterative search through the possible split indices τ to minimize $\text{Var}_{\text{intra}}$. This minimization, combined with IQR, generates τ_{split} .

We can also frame this as a problem of maximizing the variance between the two clusters, defined as *inter-split variance*, $\text{Var}_{\text{inter}}$, due to an inverse relation between $\text{Var}_{\text{inter}}$ and $\text{Var}_{\text{intra}}$; the Law of Total Variance Fisher [1958].

$$\text{Var}(U) = \text{Var}_{\text{inter}}(U_1, U_2) + \text{Var}_{\text{intra}}(U_1, U_2)$$

Hence, determining the split index that minimizes $\text{Var}_{\text{intra}}$ equates to determining the index that maximally separates clients into two distinct clusters.

This splitting to determine hard clusters is hierarchically repeated until one of these termination conditions is met: (i) reaching the minimum client threshold, η , or (ii) maximum iteration depth, T . The model then begins the next round with a randomly sampled set of clients. In the following section, we present the complete procedure in Algorithm 1.

6.3 Terraform Algorithm

We discuss the pseudo-algorithmic logic for Terraform in Algorithm 1. It takes as input a base FL algorithm \mathcal{A} , total rounds R , maximum splitting iterations T , the total client pool \mathcal{C} , client dataset sizes $|D_{\text{train}}^k|$, number of clients per round K , and minimum client threshold η . The server initializes a global model $\theta_{0,0}$ (Steps 1-3).

Each round r starts by selecting a pool of K clients, which represents the initial set of ‘hard’ clients $\mathcal{C}_{r,0}^{\mathcal{H}}$ (Steps 5-6). For each iteration t , the algorithm \mathcal{A} utilizes the current hard set $\mathcal{C}_{r,t}^{\mathcal{H}}$ and the global model $\theta_{r,t}$. It returns the set of the clients’ gradient updates, $\Delta w_{r,t}^{\mathcal{H}}$, and updated global model, $\theta_{r,t+1}$ (Step 7). This set of clients $\mathcal{C}_{r,t}^{\mathcal{H}}$ and $\Delta w_{r,t}^{\mathcal{H}}$, are then sorted according to the gradient update magnitudes, $|\Delta w_{r,t}^{\mathcal{H}}|$ (Step 8). To ensure a robust split, we find the first and third quartiles

Algorithm 1 Terraform Algorithm

```
1: Input: FL algorithm  $\mathcal{A}$ ; Rounds  $R$ ; Max. iterations  $T$ ;  
   Client set  $\mathcal{C}$ ; Client dataset size  $|D_{\text{train}}^k|$ ; No. of clients per  
   round  $K$ ; Min. clients required for splitting  $\eta$   
2: Output: Final global model  $\theta_{R,0}$   
3: Initialize: Global model  $\theta_{0,0}$   
4: for each round  $r = 0, \dots, R - 1$  do  
5:   Initialize: Randomly selected clients  $\mathcal{C}_r^K$ ; initial  
   global model  $\theta_{r,0}$ ;  
6:    $\mathcal{C}_{r,0}^{\mathcal{H}} \leftarrow \mathcal{C}_r^K$ , where  $\mathcal{H}$  : hard clients  
7:   for each splitting iteration  $t = 0, \dots, T - 1$  do  
8:      $\theta_{r,t+1}, \Delta w_{r,t}^{\mathcal{H}} \leftarrow \mathcal{A}(\theta_{r,t}, \mathcal{C}_{r,t}^{\mathcal{H}})$   
9:      $\mathcal{C}_{r,t}^{\mathcal{H}(\text{sorted})}, \Delta w_{r,t}^{\mathcal{H}(\text{sorted})} \leftarrow \text{Sort}(\mathcal{C}_{r,t}^{\mathcal{H}}, \Delta w_{r,t}^{\mathcal{H}})$   $\triangleright$   
   Sort clients  
10:     $k_{Q1}, k_{Q3} \leftarrow \text{IQR}(D_{\text{train}}^{\mathcal{H}(\text{sorted})})$   
11:     $\tau_{\text{split}} = \underset{k_{Q1} \leq \tau < k_{Q3}}{\text{argmin}} (\text{Var}_{\text{intra}}(U_1, U_2))$   
12:     $\mathcal{C}_{r,t+1}^{\mathcal{H}} \leftarrow \mathcal{C}_{r,t}^{\mathcal{H}(\text{sorted})}[\tau_{\text{split}} :]$   
13:    if  $|\mathcal{C}_{r,t+1}^{\mathcal{H}}| < \eta$  then  
14:      break  
15:    end if  
16:  end for  
17:   $\theta_{r+1,0} \leftarrow \theta_{r,t+1}$   
18: end for  
19: return  $\theta_{R,0}$ 
```

(k_{Q1}, k_{Q3}) indices using the sorted set of client data sizes, $D_{\text{train}}^{\mathcal{H}(\text{sorted})}$ (Step 9). The IQR first calculates the running sum for $D_{\text{train}}^{\mathcal{H}(\text{sorted})}$ and then calculates k_{Q1} and k_{Q3} as described in 6.2. The optimal split index τ_{split} is computed within the IQR indices (Step 10). The client set for the next iteration $\mathcal{C}_{r,t+1}^{\mathcal{H}}$ is then populated with clients ranging from the split index τ_{split} to the end of the set, $\mathcal{C}_{r,t}^{\mathcal{H}(\text{sorted})}$ (Step 11). The iterations end when client set size $< \eta$ (Steps 12-14).

The final model after T iterations is used to initialize the following round's model $\theta_{r+1,0}$ (Step 16). The output at the end of R rounds is the resulting global model $\theta_{R,0}$.

7 Evaluation

Baselines.

We evaluate Terraform against *five* state-of-the-art client selection methodologies: (i) Random Sampling i.e., FedAvg, which was presented in FedAvg; (ii) *PoC*; (iii) *Oort*; (iv) *HiCS-FL*; and (v) Baseline methodology in HiCS-FL (*HBase*), i.e., which was presented in FedProx.

FL Algorithms.

We follow prior works on client selection methodologies and test all selection methodologies on two popular FL algorithms (\mathcal{A}), FedAvg and FedProx.

Datasets.

We use the following *four* standard image classification datasets for benchmarking: (i) *CIFAR-10*: colored image dataset of objects, 10 classes Krizhevsky and Hinton [2009]; (ii) *CIFAR-100*: fine-grained version of CIFAR-10, 100

classes Krizhevsky and Hinton [2009]; (iii) *Tiny ImageNet*: colored image dataset of natural objects, 200 classes Le and Yang [2015]; and (iv) *FEMNIST*: grayscale image dataset of handwritten characters, 62 classes Caldas *et al.* [2018].

Client Models.

For CIFAR-10, each client used a 5L CNN model with 3 convolutional layers with 3×3 kernels (32/64/64 output channels), followed by two 2×2 -maxpooling layers (stride 2), a fully connected layer with 64 units, and 1D classification layer.

For CIFAR-100, each client uses a 5L CNN architecture introduced by Liu *et al.* [2024] with 2 convolutional layers with 5×5 kernel (64/128 channels), followed by 2×2 -maxpooling (stride 2) layers, followed by 3 fully connected layers (3200/256/128 units with ReLU) and a softmax classification layer. For Tiny ImageNet, we used the pre-trained ResNet18 model He *et al.* [2016].

For FEMNIST, we follow the architecture of FedAvg, i.e., the 4L CNN model with 2 convolutional layers with 5×5 kernel (32/64 channels), each with a sequential block of 2×2 -maxpooling (stride 2), followed by a 512 unit fully connected layer (ReLU), and a softmax classification layer.

Dataset Partitioning.

To simulate a realistic federated setting with statistical heterogeneity, we follow the data partitioning schemes of HiCS-FL. These schemes generate each client's local dataset using a Dirichlet distribution Yurochkin *et al.* [2019]. For example, consider 100 clients and a predefined set of five α values. Clients are divided into 20 subsets ($100/5 = 20$), with each subset chronologically assigned one of the α values. Each client in a subset receives its local data allocation through the Dirichlet distribution parameterized by its assigned α . A smaller α produces a higher class imbalance, resulting in greater heterogeneity among clients' data. Thus, given a total dataset of 1000 samples, the Dirichlet distribution assigns samples to clients according to their designated α , simulating varying levels of data heterogeneity across the client set.

We use HiCS-FL partitioning scenarios.

FEMNIST uses 50-100 clients, and its following 8 scenarios are based on 5 α values and 3 sampling rates. Scenarios for sampling rate = 0.1, 50 clients, **(1)**: $\alpha = \{0.001, 0.002, 0.005, 0.01, 0.5\}$, **(2)**: $\alpha = \{0.001, 0.002, 0.005, 0.01, 0.2\}$, and **(3)**: $\alpha = \{0.001\}$. Scenarios for sampling rate = 0.3, 50 clients, **(1*)**: $\alpha = \{0.001, 0.002, 0.005, 0.01, 0.5\}$, **(2*)**: $\alpha = \{0.001, 0.002, 0.005, 0.01, 0.2\}$, and **(3*)**: $\alpha = \{0.001\}$. Scenarios for sampling rate = 0.15, 100 clients, **(4)**: $\alpha = \{0.1, 0.1, 0.1, 0.3, 0.3\}$, and **(5)**: $\alpha = \{0.05, 0.1, 0.15, 0.2, 0.25, 0.3, 0.35, 0.4, 0.45, 0.5\}$.

CIFAR-10 uses 50 clients, and its following 3 scenarios are based on sampling rate = 0.2 and 3 α values. **(1)**: $\alpha = \{0.001, 0.01, 0.1, 0.5, 1\}$, **(2)**: $\alpha = \{0.001, 0.002, 0.005, 0.01, 0.5\}$, and **(3)**: $\alpha = \{0.001, 0.002, 0.005, 0.01, 0.1\}$.

As HiCS-FL does not evaluate on datasets CIFAR-100, Tiny ImageNet, and FEMNIST, we use the following scenarios: CIFAR-100 uses 250 clients and sampling rate = 0.128, whereas Tiny ImageNet uses 500 clients and sampling rate = 0.058; $\alpha = 0.1$ for both. FEMNIST has a total of 800k+ samples, and these samples were assigned among 3597 clients

Table 1: Accuracy of client models with **best** and **second-best** methodologies highlighted.

\mathcal{A}	Methodology	CIFAR-10			CIFAR-100	Tiny ImageNet	FEMNIST
		1	2	3			
FedAvg	Random	<u>67.76%</u>	58.21%	54.69%	15.26%	35.44%	81.28%
	HBase	54.76%	41.09%	41.69%	15.58%	35.99%	79.44%
	PoC	47.84%	27.37%	24.51%	13.73%	34.29%	80.31%
	HiCS-FL	65.57%	57.24%	<u>57.00%</u>	16.38%	<u>36.09%</u>	<u>81.46%</u>
	Oort	65.41%	<u>60.20%</u>	54.71%	<u>16.43%</u>	35.05%	80.38%
	Terraform (Ours)	68.23%	63.23%	57.10%	24.22%	42.34%	83.37%
FedProx	Random	<u>66.17%</u>	<u>60.01%</u>	52.47%	15.97%	<u>35.46%</u>	81.28%
	HBase	55.90%	41.21%	43.79%	16.71%	35.10%	81.49%
	PoC	47.33%	20.28%	28.00%	13.81%	34.99%	80.31%
	HiCS-FL	67.10%	58.59%	<u>57.94%</u>	<u>17.54%</u>	35.36%	81.08%
	Oort	65.83%	58.58%	54.58%	<u>17.54%</u>	35.31%	80.59%
	Terraform (Ours)	68.52%	62.73%	59.13%	24.81%	42.44%	83.52%

Table 2: Accuracy of client models for FMNIST scenarios with **best** and **second-best** methodologies highlighted.

\mathcal{A}	Methodology	1	2	3	1*	2*	3*	4	5
FedAvg	Random	85.62%	<u>83.28%</u>	70.19%	<u>84.05%</u>	83.84%	70.15%	85.18%	84.78%
	HBase	74.23%	71.20%	71.69%	80.74%	83.11%	73.15%	85.36%	85.70%
	PoC	80.29%	79.36%	58.11%	81.93%	83.17%	53.40%	85.32%	84.93%
	HiCS-FL	<u>87.14%</u>	82.81%	68.14%	83.60%	84.32%	71.18%	<u>85.39%</u>	85.16%
	Oort	89.01%	85.42%	59.52%	83.21%	<u>84.75%</u>	57.39%	85.09%	<u>85.79%</u>
	Terraform (Ours)	85.62%	<u>83.28%</u>	70.19%	85.49%	85.47%	<u>71.21%</u>	86.08%	86.51%
FedProx	Random	85.78%	<u>83.24%</u>	<u>70.97%</u>	83.27%	83.99%	70.01%	85.22%	85.10%
	HBase	76.23%	72.39%	72.11%	81.35%	83.07%	71.37%	85.75%	<u>85.70%</u>
	PoC	84.50%	79.67%	59.42%	82.22%	83.08%	65.42%	85.44%	84.99%
	HiCS-FL	86.00%	80.61%	69.48%	83.41%	<u>85.10%</u>	69.71%	<u>85.77%</u>	84.84%
	Oort	87.11%	85.43%	59.42%	83.47%	84.69%	66.79%	85.47%	85.51%
	Terraform (Ours)	85.78%	<u>83.24%</u>	<u>70.97%</u>	83.91%	85.75%	<u>70.02%</u>	87.24%	86.63%

using the writer ID Li *et al.* [2020] partitioning. We used a sampling rate of 0.011.

Setup.

We use NVIDIA’s A100 Tensor Core GPUs to run our experiments. Each result is averaged over three runs to eliminate any noise.

We follow HiCS-FL and FedProx and set the hyperparameter μ of the regularization term of FedProx to 0.1. For FMNIST dataset, we use the stochastic gradient descent (SGD) optimizer. The learning rate is initially set to 0.001 and decreases every 10 iterations with a decay factor of 0.5. The global communication rounds is set to 200. The number of local epochs is set to 2 and the size of a mini-batch is set to 64. For datasets CIFAR-10, CIFAR-100, and Tiny ImageNet, we use the popular optimizer Adam Kingma and Ba [2015] with a learning rate of 0.001 (0.01 for Tiny ImageNet), a decay factor of 0.5, global communication rounds of 100 (500 for CIFAR-10), local epochs of 2, and a mini-batch size of 64. For FEMNIST, we use SGD optimizer with a learning rate of 0.01, local epochs of 5, and a mini-batch size of 32.

7.1 Results

We now illustrate the results of comparing Terraform against other client selection methodologies. We use Tables 1 and 2 to illustrate the average accuracy of the global model on the test data of the participating clients using FL algorithms.

In Table 1, we observe that Terraform yields the highest accuracy among all the methodologies for all cases. For CIFAR-10, as expected, the accuracy for all methodologies decreases with increasing heterogeneity. Consequently, on

FedAvg, we observe that Oort and HiCS-FL yield better accuracy than Random for scenarios 2 and 3, and HiCS-FL does better than Oort on scenario 3 due to its heterogeneity-focused client clustering. *Note:* for CIFAR-10 and FMNIST, we follow the three scenarios of HiCS-FL (1, 2, and 3), which restrict us to initially sample only 10 and 5 clients, respectively. If Terraform is allowed to sample more initial clients in each round, it can yield higher accuracy, which is evident in Table 2 (4 and 5). However, on FedProx, Random outperforms others on scenario 2 because FedProx’s high regularization factor ($\mu = 0.1$) leads to underfitting.

On Tiny ImageNet and CIFAR-100, Terraform shines the most; it achieves up to 17.31% and 47.41% more accuracy than the second-best methodology as it allowed to sample a higher number of clients initially in each round. Although a similar trend for Terraform exists on FEMNIST, we attribute it to more classes in the dataset, which increases non-iid relationships, and increase the data heterogeneity.

In Table 2, we evaluate Terraform on 8 FMNIST scenarios. As scenarios 1, 2, and 3 are ported from HiCS-FL, we force Terraform to sample only 5 clients initially. Consequently, Terraform is able to run only one iteration per round, which is same as running Random; thus, similar accuracies. For rest of the scenarios, Terraform does not have this restriction, and thus, it continues outperforming other methodologies. One exception, however, is scenario 3*, where Terraform is the second-best because sampling even 15 clients initially, in each round, is not sufficient; we hypothesize that Terraform needs to sample a much higher number of clients.

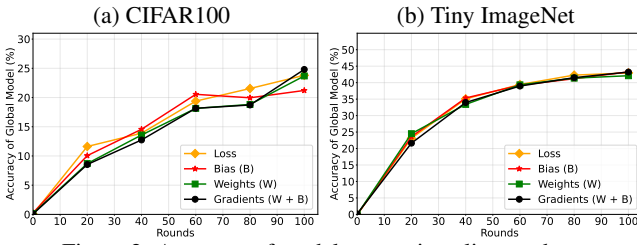


Figure 2: Accuracy of model on varying client updates.

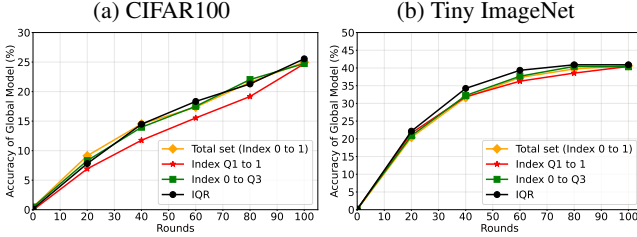


Figure 3: Accuracy of global model on varying quartiles.

7.2 Ablation Studies

We validate Terraform’s contribution through ablation studies that assess the efficacy of client updates, IQR, and client threshold (η) in client selection.

Varying Client Updates.

Terraform’s gradient updates are, in essence, a combination of the weights and biases from the clients’ models’ final layers. In Figure 2, we illustrate the accuracy of Terraform when, instead of using gradient updates, it uses (i) loss, (ii) biases, and (iii) weights.

We observe that using gradient updates (weights + bias) with Terraform yields the best performance at the end of 100 rounds of training for both CIFAR-100 and Tiny ImageNet. Moreover, using biases, which is a HiCS-FL approach, has the lowest performance for the CIFAR-100 dataset compared to the Tiny ImageNet due to the reduced number of classes in the former dataset. This, in turn, reduces the bias values per client, thereby affecting the representative values for the client’s distribution.

Varying Quartiles.

To determine the optimal split index τ_{split} , Terraform searches in its Inter-Quartile Range (IQR) for an index that minimizes the intra-split variance (Var_{intra}). A brute-force approach to determine the split index τ_{split} is to iterate over each index in the set of client dataset sizes, $D_{train}^{\mathcal{H}(\text{sorted})}$, and calculate the intra-split variance. Such an approach would be computationally expensive, and IQR minimizes this cost by reducing the search space: from the total set (0,1) to the region between the first and third quartiles of the set (Q1, Q3).

In Figure 3, on the CIFAR100 and Tiny ImageNet datasets for 100 rounds, we compare IQR (Q1, Q3) against three other splitting ranges: (0, 1), (0, Q3), and (Q1, 1). Our results illustrate that IQR is not only sufficient for determining split index τ_{split} , but also helps to discard outliers that reduce the test accuracy. Additionally, (Q3, 1) have the poorest performance, which validates the theory that hyper-focusing on only highly

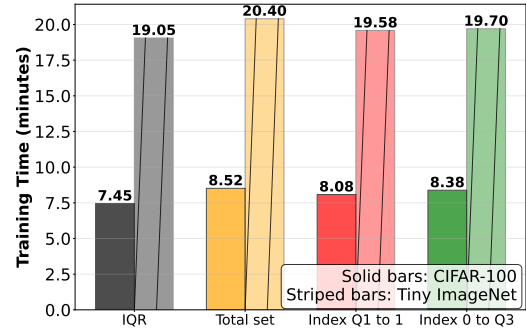


Figure 4: Training time on varying quartiles.

Table 3: Accuracy on varying thresholds, η .

Dataset	$\eta = 2$	$\eta = 3$	$\eta = 4$
FEMNIST	83.61%	83.15%	83.52%
FMNIST(1*)	80.26%	82.58%	83.91%
FMNIST(4)	86.07%	86.51%	87.24%

heterogeneous clients overfits the model and reduces generalization.

Training time: In Figure 4, we measure the training time complexity for the 4 quartile ranges and observe that our claims that IQR and total set have the lowest and highest training time, respectively, hold.

Threshold for #Clients (η).

Terraform’s hierarchical sampling approach iteratively splits the set of clients into easy \mathcal{E} and hard \mathcal{H} clusters. Specifically, we keep splitting the hard cluster until the following termination condition is met: the size of the hard cluster falls below a predefined threshold (η). Determining an optimal value of η saves compute as further splitting will yield minimal benefits. Thus, we set η to 4. In Table 3, we illustrate the accuracy on three different values for $\eta = \{2, 3, 4\}$ on FEMNIST and FMNIST (1 and 4*) scenarios. We observe that $\eta = 4$ performs well on both datasets. Although $\eta = 2$ yields a marginally better accuracy on the FEMNIST dataset, $\eta = 4$ reduces the computational cost for training and yields only 0.11% lower accuracy than $\eta = 2$, which makes it an optimal choice.

8 Conclusions

In this paper, we presented Terraform, a novel client selection methodology that mitigates the impact of heterogeneous clients on federated learning. Terraform achieves this goal by hierarchically selecting and retraining heterogeneous clients. Terraform performs this hierarchical selection on the basis of clients’ local model’s final-layer gradient updates, which it uses to determine the optimal inter-quartile range (IQR) to split clients into easy and hard clusters. Terraform retrains clients in hard clusters and our results illustrate that it outperforms existing works by up to 47%.

References

Durmus Alp Emre Acar, Yue Zhao, Ramon Matas, Matthew Mattina, Paul Whatmough, and Venkatesh Saligrama. Fed-

- erated learning based on dynamic regularization. In *International Conference on Learning Representations*, 2021.
- Manoj Ghuhan Arivazhagan, Vinay Aggarwal, Aaditya Kumar Singh, and Sunav Choudhary. Federated learning with personalization layers. *arXiv preprint arXiv:1912.00818*, 2019.
- Ravikumar Balakrishnan, Tian Li, Tianyi Zhou, Nageen Himayat, Virginia Smith, and Jeff Bilmes. Diverse client selection for federated learning via submodular maximization. In *International Conference on Learning Representations*, 2022.
- L. Breiman, J. Friedman, C.J. Stone, and R.A. Olshen. *Classification and Regression Trees*. Taylor & Francis, 1984.
- Sebastian Caldas, Sai Meher Karthik Duddu, Peter Wu, Tian Li, Jakub Konečný, H Brendan McMahan, Virginia Smith, and Ameet Talwalkar. Leaf: A benchmark for federated settings. *arXiv preprint arXiv:1812.01097*, 2018.
- Hong-You Chen and Wei-Lun Chao. On bridging generic and personalized federated learning for image classification. In *International Conference on Learning Representations*, 2022.
- Huancheng Chen and Haris Vikalo. Heterogeneity-guided client sampling: Towards fast and efficient non-iid federated learning. *Advances in Neural Information Processing Systems*, 37:65525–65561, 2024.
- Weiyu Cheng, Yanyan Shen, Yanmin Zhu, and Linpeng Huang. A neural attention model for urban air quality inference: Learning the weights of monitoring stations. In *Proceedings of the AAAI conference on artificial intelligence*, volume 32, 2018.
- Liam Collins, Hamed Hassani, Aryan Mokhtari, and Sanjay Shakkottai. Exploiting shared representations for personalized federated learning. In *International conference on machine learning*, pages 2089–2099. PMLR, 2021.
- Alireza Fallah, Aryan Mokhtari, and Asuman Ozdaglar. Personalized federated learning with theoretical guarantees: A model-agnostic meta-learning approach. *Advances in neural information processing systems*, 33:3557–3568, 2020.
- Federal Emergency Management Agency. The rural fire problem in the united states. <https://www.usfa.fema.gov/downloads/pdf/statistics/rural.pdf>, 1997. United States Fire Administration report.
- Ronald Fisher. *Statistical Methods for Research Workers*. Oliver and Boyd, Edinburgh, thirteenth edition, 1958.
- Yann Fraboni, Richard Vidal, Laetitia Kameni, and Marco Lorenzi. Clustered sampling: Low-variance and improved representativity for clients selection in federated learning. In *International Conference on Machine Learning*, pages 3407–3416. PMLR, 2021.
- Stefano Galmarini and S Trivikrama Rao. The aqmeii two-continent regional air quality model evaluation study: Fueling ideas with unprecedented data. *Atmospheric Environment*, 45(14):2464, 2011.
- Liang Gao, Huazhu Fu, Li Li, Yingwen Chen, Ming Xu, and Cheng-Zhong Xu. Feddc: Federated learning with non-iid data via local drift decoupling and correction. In *Proceedings of the IEEE/CVF conference on computer vision and pattern recognition*, pages 10112–10121, 2022.
- Avishek Ghosh, Jichan Chung, Dong Yin, and Kannan Ramchandran. An efficient framework for clustered federated learning. *Advances in neural information processing systems*, 33:19586–19597, 2020.
- G.H. Golub and C.F. Van Loan. *Matrix Computations*. Johns Hopkins Studies in the Mathematical Sciences. Johns Hopkins University Press, 1996.
- Dennis Grinwald, Philipp Wiesner, and Shinichi Nakajima. Federated learning over connected modes. *Advances in Neural Information Processing Systems*, 37:85179–85202, 2024.
- T. Hastie, R. Tibshirani, and J.H. Friedman. *The Elements of Statistical Learning: Data Mining, Inference, and Prediction*. Springer series in statistics. Springer, 2001.
- Kaiming He, Xiangyu Zhang, Shaoqing Ren, and Jian Sun. Deep residual learning for image recognition. In *Proceedings of the IEEE conference on computer vision and pattern recognition*, pages 770–778, 2016.
- Md Sirajul Islam, Simin Javaherian, Fei Xu, Xu Yuan, Li Chen, and Nian-Feng Tzeng. Fedclust: Tackling data heterogeneity in federated learning through weight-driven client clustering. In *Proceedings of the 53rd International Conference on Parallel Processing*, pages 474–483, 2024.
- Yae Jee Cho, Jianyu Wang, and Gauri Joshi. Towards understanding biased client selection in federated learning. In Gustau Camps-Valls, Francisco J. R. Ruiz, and Isabel Valera, editors, *Proceedings of The 25th International Conference on Artificial Intelligence and Statistics*, volume 151 of *Proceedings of Machine Learning Research*, pages 10351–10375. PMLR, 28–30 Mar 2022.
- Yihan Jiang, Jakub Konečný, Keith Rush, and Sreeram Kannan. Improving federated learning personalization via model agnostic meta learning. *ArXiv*, abs/1909.12488, 2019.
- Xiaowen Jiang, Anton Rodomanov, and Sebastian U Stich. Federated optimization with doubly regularized drift correction. In *Forty-first International Conference on Machine Learning*, 2024.
- Hu Jin and Jun Du. Federated learning based fire detection method using local mobilenet. *Frontiers in Public Health*, 12:1280250, 2024.
- Sai Praneeth Karimireddy, Satyen Kale, Mehryar Mohri, Sashank Reddi, Sebastian Stich, and Ananda Theertha Suresh. Scaffold: Stochastic controlled averaging for federated learning. In *International conference on machine learning*, pages 5132–5143. PMLR, 2020.
- Diederik P. Kingma and Jimmy Ba. Adam: A method for stochastic optimization. *International Conference on Learning Representations (ICLR)*, 2015.

- Alex Krizhevsky and Geoffrey Hinton. Learning multiple layers of features from tiny images. Technical report, University of Toronto, 2009.
- Fan Lai, Xiangfeng Zhu, Harsha V Madhyastha, and Mosharaf Chowdhury. Oort: Efficient federated learning via guided participant selection. In *15th {USENIX} Symposium on Operating Systems Design and Implementation ({OSDI} 21)*, pages 19–35, 2021.
- Yann Le and Xuan Yang. Tiny imagenet visual recognition challenge. *CS 231N*, 7(7):3, 2015.
- Daliang Li and Junpu Wang. Fedmd: Heterogenous federated learning via model distillation. *arXiv preprint arXiv:1910.03581*, 2019.
- Tian Li, Anit Kumar Sahu, Manzil Zaheer, Maziar Sanjabi, Ameet Talwalkar, and Virginia Smith. Federated optimization in heterogeneous networks. *Proceedings of Machine learning and systems*, 2:429–450, 2020.
- Qinbin Li, Bingsheng He, and Dawn Song. Model-contrastive federated learning. In *Proceedings of the IEEE/CVF conference on computer vision and pattern recognition*, pages 10713–10722, 2021.
- Tian Li, Shengyuan Hu, Ahmad Beirami, and Virginia Smith. Ditto: Fair and robust federated learning through personalization. In *International conference on machine learning*, pages 6357–6368. PMLR, 2021.
- Paul Pu Liang, Terrance Liu, Ziyin Liu, Ruslan Salakhutdinov, and Louis-Philippe Morency. Think locally, act globally: Federated learning with local and global representations. *ArXiv*, abs/2001.01523, 2019.
- Xianfeng Liang, Shuheng Shen, Jingchang Liu, Zhen Pan, Yifei Cheng, and Enhong Chen. Variance reduced local {sgd} with lower communication complexity, 2020.
- Tao Lin, Lingjing Kong, Sebastian U Stich, and Martin Jaggi. Ensemble distillation for robust model fusion in federated learning. *Advances in neural information processing systems*, 33:2351–2363, 2020.
- Zhexiong Liu, Licheng Liu, Yiqun Xie, Zhenong Jin, and Xiaowei Jia. Task-adaptive meta-learning framework for advancing spatial generalizability. In *Proceedings of the AAAI Conference on Artificial Intelligence*, volume 37, pages 14365–14373, 2023.
- Renpu Liu, Cong Shen, and Jing Yang. Federated representation learning in the under-parameterized regime. In *Forty-first International Conference on Machine Learning*, 2024.
- Google LLC. Google nest protect (2nd gen) smoke and co detector, 2025. Accessed August 21, 2025.
- Brendan McMahan, Eider Moore, Daniel Ramage, Seth Hampson, and Blaise Aguerre y Arcas. Communication-efficient learning of deep networks from decentralized data. In *Artificial intelligence and statistics*, pages 1273–1282. PMLR, 2017.
- National Interagency Fire Center (NIFC) National Interagency Coordination Center (NICC). Wildland fire summary and statistics annual report 2024, 2024. Accessed August 21, 2025.
- Takayuki Nishio and Ryo Yonetani. Client selection for federated learning with heterogeneous resources in mobile edge. In *ICC 2019-2019 IEEE international conference on communications (ICC)*, pages 1–7. IEEE, 2019.
- U.S. Department of Homeland Security. Fema smartphone application with disaster reporter feature - privacy impact assessment. Privacy impact assessment, Department of Homeland Security, 2013.
- Jaehoon Oh, SangMook Kim, and Se-Young Yun. FedBABU: Toward enhanced representation for federated image classification. In *International Conference on Learning Representations*, 2022.
- Zhengxiang Pan, Han Yu, Chunyan Miao, and Cyril Leung. Crowdsensing air quality with camera-enabled mobile devices. In *Proceedings of the AAAI conference on artificial intelligence*, volume 31, pages 4728–4733, 2017.
- Xingchao Peng, Zijun Huang, Yizhe Zhu, and Kate Saenko. Federated adversarial domain adaptation. In *International Conference on Learning Representations*, 2020.
- O. Raffeg et al. Legal and ethical considerations for demand-driven data collection in disasters. *International Journal of Disaster Risk Reduction*, 2025. Available online.
- Sashank J. Reddi, Zachary Charles, Manzil Zaheer, Zachary Garrett, Keith Rush, Jakub Konečný, Sanjiv Kumar, and Hugh Brendan McMahan. Adaptive federated optimization, 2021.
- Pacific Rivers and Portland State University. Impact of four oregon fires on drinking water systems, 2022. Accessed August 21, 2025.
- Felix Sattler, Klaus-Robert Müller, and Wojciech Samek. Clustered federated learning: Model-agnostic distributed multitask optimization under privacy constraints. *IEEE transactions on neural networks and learning systems*, 32(8):3710–3722, 2020.
- Jonathan Scott, Hossein Zakerinia, and Christoph H Lampert. PeFLL: Personalized federated learning by learning to learn. In *The Twelfth International Conference on Learning Representations*, 2024.
- Aviv Shamsian, Aviv Navon, Ethan Fetaya, and Gal Chechik. Personalized federated learning using hypernetworks. In *International Conference on Machine Learning*, 2021.
- Changlong Shi, He Zhao, Bingjie Zhang, Mingyuan Zhou, Dandan Guo, and Yi Chang. Fedawa: Adaptive optimization of aggregation weights in federated learning using client vectors. In *Proceedings of the Computer Vision and Pattern Recognition Conference*, pages 30651–30660, 2025.
- K. Smith, G. Kent, D. Slater, G. Plank, M. Williams, M. McCarthy, F. Vernon, N. Driscoll, and H.-W. Braun. Integrated multi-hazard regional networks: Earthquake warning/response, wildfire detection/response, and extreme weather tracking. In Robert Anderson and Horacio Ferriz, editors, *Special Volume: Association of Environmental*

- and Engineering Geologists, *Applied Geology in California*, pages 599–612. Association of Environmental and Engineering Geologists, 2016.
- Canh T Dinh, Nguyen Tran, and Josh Nguyen. Personalized federated learning with moreau envelopes. *Advances in neural information processing systems*, 33:21394–21405, 2020.
- Yue Tan, Guodong Long, Lu Liu, Tianyi Zhou, Qinghua Lu, Jing Jiang, and Chengqi Zhang. Fedproto: Federated prototype learning across heterogeneous clients. In *AAAI Conference on Artificial Intelligence*, 2021.
- Andrew S. Tanenbaum and Maarten van Steen. *Distributed Systems: Principles and Paradigms*. Pearson Prentice Hall, Upper Saddle River, NJ, 2nd edition, 2007.
- Minxue Tang, Xuefei Ning, Yitu Wang, Jingwei Sun, Yu Wang, Hai Li, and Yiran Chen. Fedcor: Correlation-based active client selection strategy for heterogeneous federated learning. In *Proceedings of the IEEE/CVF Conference on Computer Vision and Pattern Recognition*, pages 10102–10111, 2022.
- Yitong Tang. Adapted weighted aggregation in federated learning. In *Proceedings of the AAAI Conference on Artificial Intelligence*, volume 38, pages 23763–23765, 2024.
- Reno University of Nevada, San Diego University of California, and University of Oregon. Alertwildfire camera system, 2025. Accessed August 21, 2025.
- U.S. Department of Homeland Security. Privacy compliance review of the federal emergency management agency information sharing, 2019.
- Mike Wall and Space.com. Here’s why nasa wants your photos of hurricane damage, 2025. Yahoo News, August 21, 2025.
- Hongyi Wang, Mikhail Yurochkin, Yuekai Sun, Dimitris Papailiopoulos, and Yasaman Khazaeni. Federated learning with matched averaging. In *International Conference on Learning Representations*, 2020.
- Jianyu Wang, Qinghua Liu, Hao Liang, Gauri Joshi, and H Vincent Poor. Tackling the objective inconsistency problem in heterogeneous federated optimization. *Advances in neural information processing systems*, 33:7611–7623, 2020.
- Shuai Wang, Yanqing Xu, Zhiguo Wang, Tsung-Hui Chang, Tony QS Quek, and Defeng Sun. Beyond admm: A unified client-variance-reduced adaptive federated learning framework. In *Proceedings of the AAAI Conference on Artificial Intelligence*, volume 37, pages 10175–10183, 2023.
- Hongda Wu and Ping Wang. Fast-convergent federated learning with adaptive weighting. *IEEE Transactions on Cognitive Communications and Networking*, 7(4):1078–1088, 2021.
- Yiqun Xie, Erhu He, Xiaowei Jia, Han Bao, Xun Zhou, Rahul Ghosh, and Praveen Ravirathinam. A statistically-guided deep network transformation and moderation framework for data with spatial heterogeneity. In *2021 IEEE International Conference on Data Mining (ICDM)*, pages 767–776. IEEE, 2021.
- Jian Xu, Xinyi Tong, and Shao-Lun Huang. Personalized federated learning with feature alignment and classifier collaboration. In *The Eleventh International Conference on Learning Representations*, 2023.
- Qiang Yang, Yang Liu, Tianjian Chen, and Yongxin Tong. Federated machine learning: Concept and applications. *ACM Transactions on Intelligent Systems and Technology (TIST)*, 10(2):12:1–12:19, 2019.
- Zhiqin Yang, Yonggang Zhang, Yu Zheng, Xinmei Tian, Hao Peng, Tongliang Liu, and Bo Han. Fedfed: Feature distillation against data heterogeneity in federated learning. In A. Oh, T. Naumann, A. Globerson, K. Saenko, M. Hardt, and S. Levine, editors, *Advances in Neural Information Processing Systems*, volume 36, pages 60397–60428. Curran Associates, Inc., 2023.
- Xiyuan Yang, Wenke Huang, and Mang Ye. Fedas: Bridging inconsistency in personalized federated learning. In *Proceedings of the IEEE/CVF Conference on Computer Vision and Pattern Recognition*, pages 11986–11995, 2024.
- Tehrim Yoon, Sumin Shin, Sung Ju Hwang, and Eunho Yang. Fedmix: Approximation of mixup under mean augmented federated learning. In *International Conference on Learning Representations*, 2021.
- Mikhail Yurochkin, Mayank Agarwal, Soumya Ghosh, Kristjan Greenewald, Nghia Hoang, and Yasaman Khazaeni. Bayesian nonparametric federated learning of neural networks. In *International conference on machine learning*, pages 7252–7261. PMLR, 2019.
- Matthew D Zeiler and Rob Fergus. Visualizing and understanding convolutional networks. In *European conference on computer vision*, pages 818–833. Springer, 2014.